

# Chondritic Meteorite Fragments Associated with the Permian-Triassic Boundary in Antarctica

Asish R. Basu,<sup>1\*</sup> Michail I. Petaev,<sup>2,3</sup> Robert J. Poreda,<sup>1</sup> Stein B. Jacobsen,<sup>2</sup> Luann Becker<sup>4</sup>

Multiple chondritic meteorite fragments have been found in two sedimentary rock samples from an end-Permian bed at Graphite Peak in Antarctica. The Ni/Fe, Co/Ni, and P/Fe ratios in metal grains; the Fe/Mg and Mn/Fe ratios in olivine and pyroxene; and the chemistry of Fe-, Ni-, P-, and S-bearing oxide in the meteorite fragments are typical of CM-type chondritic meteorites. In one sample, the meteoritic fragments are accompanied by more abundant discrete metal grains, which are also found in an end-Permian bed at Meishan, southern China. We discuss the implications of this finding for a suggested global impact event at the Permian-Triassic boundary.

Meteorite samples that occur as fragments in Earth rocks are rare. There are only a few examples in the literature of which two are deep-sea drill core occurrences. One includes fragments of an achondrite, the Eltanin meteorite (1). A feldspar from this material was so well preserved that it yielded a present  $^{87}\text{Sr}/^{86}\text{Sr} = 0.699013 \pm 11$ , only slightly higher than the initial solar system value. The second is a 2.5-mm-size meteorite (2) from the Cretaceous-Tertiary (K-T) boundary layer of a North Pacific deep-sea drill core that resembles a carbonaceous chondrite and is interpreted as a remnant of the K-T impactor of 65 million years ago (3). Ordinary chondrite remnants were also reported from carbonate rocks of southern Sweden, where the surviving mineral is believed to be chromite (4, 5). This paper describes the discovery of chondritic meteorite fragments and metallic grains in the end-Permian strata at Graphite Peak, Central Transantarctic Mountains, Antarctica (Fig. 1) and confirms a previous report of metallic grains from the end-Permian boundary in Meishan (6), southern China (Fig. 1). It has been suggested (6) that the metallic grains from Meishan may have condensed from an impact-generated vapor cloud, although this suggestion is yet to gain acceptance.

Graphite Peak, Antarctica (Fig. 1), exposes a 550-m continuous section of the Buckley and Fremouw formations (7, 8). The end-Permian

beds are exposed over about 2 m and include the last Gondwana coal bed of end-Permian age, above a bed with the last occurrence of *Glossopteris* flora. Above the coal bed is a claystone breccia with anomalously low  $\delta^{13}\text{C}$  value ( $\sim -40$ ‰). Shocked quartz (8) and extraterrestrial fullerenes with trapped noble gases have been reported from this bed (9). On the basis of paleobotanic and isotopic criteria, and shocked quartz grains, the claystone breccia (Fig. 1) has been identified as the Permian-Triassic (P-T) boundary in Antarctica (7, 8, 10). This interpretation was also confirmed and extended by similar observations on P-T sections at Wybung Head, NSW, Australia (7, 10), as well as by extraterrestrial fullerene evidence from China and Japan (11). The aforementioned findings provided a strong rationale to undertake a thorough petrological-mineralogical study of the magnetic grains from some of these end-Permian sedimentary rocks. Specifically, high  $^3\text{He}$ -bearing magnetic grains and their unique noble gas signatures (9) from the Graphite Peak P-T boundary needed to be fully evaluated in the context of a potential-impact tracer. These rock samples used in the previous study (9) were available in our laboratories. Therefore, we examined four samples of Graphite Peak claystone breccia at the P-T boundary [three of these are subsamples of no. 2060 from (8), and one is no. 315 from (7)] and another claystone-shale sample [sample no. 2064 of (8)],  $\sim 0.8$  m below the boundary layer (Fig. 1). We also examined a sample of the reddish-black sediment layer believed to mark the end-Permian at Meishan, China (6, 12), where Fe-Ni-Si grains were reported earlier from the same layer (6).

We separated magnetic particles from these P-T boundary samples at Graphite Peak, Antarctica, and Meishan, China. The magnetic particles from Meishan are opaque and variable in size (20 to 200  $\mu\text{m}$ ). The outlines of these grains are irregular, curved

and subrounded (Fig. 2A) and strongly resemble the so-called "native-iron nuggets" reported from the bedded chert layer of the Permo-Triassic section in Sasayama, Japan (13). Most of the grains from our Meishan sample are compositionally similar to the Fe-Ni-Si grains reported previously (6) from the base of bed 25 marking the end-Permian in the Meishan section. Our electron microprobe measurements (14) show that the grains are almost pure Fe (99 to 100%) with up to 0.20 weight % Ni, 0.60 weight % Cr, and 0.39 weight % Si.

The magnetic fraction from the claystone breccia at the P-T boundary of Graphite Peak consists of abundant opaque grains and rare aggregates of silicates and opaque minerals. Three types of opaque grains were identified in the Graphite Peak samples: (i) predominant Fe-rich metal nuggets, (ii) less abundant Fe, Ni, P, S-bearing oxides, and (iii) rare Fe, Ni-sulfides. The pure metal grains that are common in the Meishan boundary layer are also abundant ( $\sim 70\%$ ) among the Graphite Peak opaque grains (Fig. 2B). These grains are similar but more diverse in composition

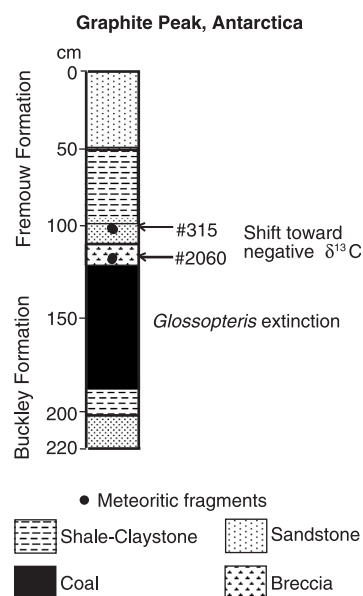


**Fig. 1.** Lithostratigraphy of the P-T boundary, as defined isotopically and paleobotanically (7, 8) in Graphite Peak near Beardmore Glacier, Central Transantarctic Mountains. This figure shows the relative positions of two samples of the meteoritic fragments containing claystone breccia, no. 2060 from the base and no. 315 from 23 cm above. The claystone breccia rests directly above the coal horizon with the last occurrence of *Glossopteris* (8). Fullerenes containing extraterrestrial  $^3\text{He}$  (9) along with shocked quartz grains and a negative shift in  $\delta^{13}\text{C}$  were reported (7, 8) earlier from the horizon containing these meteorite-bearing samples. Our discovery of the meteorite fragments in these rocks, along with previous evidence referred to above (7–9), indicates that the claystone breccia is a rapidly redeposited unit, in part from distant impact fallouts.

<sup>1</sup>Department of Earth and Environmental Sciences, University of Rochester, Rochester, NY 14627, USA.

<sup>2</sup>Department of Earth and Planetary Sciences, Harvard University, Cambridge, MA 02138, USA. <sup>3</sup>Harvard-Smithsonian Center for Astrophysics, 60 Garden Street, Cambridge, MA 02138, USA. <sup>4</sup>Institute of Crustal Studies, Department of Geology, University of California, Santa Barbara, CA 93106, USA.

\*To whom correspondence should be addressed. E-mail: abasu@earth.rochester.edu

than those in Meishan and range in Fe compositions up to 100%, with variable amounts of Ni (up to 0.16%), Cr (up to 12.48%), and Si (up to 2.62%). The common occurrence of Fe-Ni-Si grains at the Graphite Peak P-T boundary layer and at the P-T event stratigraphic layer (15, 16) in Meishan provides further evidence that we have sampled the P-T boundary at Graphite Peak. These “event-marker” magnetic grains occur only in the boundary layer and are absent in samples above and below, at Meishan (6). Our study of the magnetic fraction of the bed 0.8 m below the P-T boundary at Graphite Peak yielded only terrestrial Fe oxides and hydroxides, lacking Ni, S, and P.

In the magnetic fractions of the Graphite Peak samples no. 2060 and no. 315, we also found a number of particles enriched in silicate minerals. The results of our electron microprobe study of these particles (14) are summarized in Tables 1 and 2 and

the supporting online material (tables S1 to S4 and figs. S1 and S2). All fragments display identical poikilitic or granular textures (Fig. 3, A to D). They contain small euhedral-to-subhedral forsterite grains enclosed in larger grains of clinoenstatite, which shows clear polysynthetic twinning in one of the fragments (Fig. 3D). The chemical compositions of forsterite and clinoenstatite (Table 1) show low concentrations of FeO and relatively high Mn/Fe ratios. Such compositions do not occur in terrestrial olivines and pyroxenes and are indicative of an extraterrestrial origin. Forsterite has rather high concentrations of CaO and Cr<sub>2</sub>O<sub>3</sub>, characteristic of some chondritic meteorites (17). Two minor silicate phases, Ca-rich clinopyroxene and Al-rich mesostasis, usually occur as interstitial anhedral patches. The composition of mesostasis (Table 1) varies from Ol-normative to An-normative and the low Na<sub>2</sub>O content is similar to those of type I chondrules. The Ca-rich clinopyroxenes display a wide range of CaO content from pigeonite to subcalcic augite. As do forsterite and clinoenstatite, they have low FeO content and high Mn/Fe ratios up to ~2 in two grains of MnO-rich augites (Table 1). We conclude that the magnetic silicate aggregates are meteorite fragments. A total of 20

such meteorite fragments have been identified in two of the subsamples of no. 2060 and several dozens of smaller meteorite fragments or mineral grains in no. 315 (see supporting online material, figs. S1 and S2).

The meteorite fragments contain abundant Fe-rich opaque phases, which make the whole fragments magnetic. The electron microprobe study revealed three major types of opaque phases: (i) Fe,Ni,P,S-bearing oxides, (ii) Fe,Ni,Co,P,Cr-bearing metal grains, and (iii) Fe,Ni-sulfides. The Fe, Ni,P,S-oxides (Fig. 3, A to C) tend to form rounded blobs or irregular masses often interconnected by thin veins of the same material. In back-scattered and secondary electron images, these masses display highly irregular surfaces with numerous pits and caverns indicative of the polymineralic nature of these materials. The high concentrations of Ni, P, and S in their chemical compositions along with the low analytical totals (Table 2) suggest that the Fe,Ni,P,S-oxides are the polymineralic aggregates of Fe oxides or hydroxides, Fe,Ni sulfides, and Fe,Ni phosphides or -phosphates likely formed by weathering (in the meteorite parent body) of a primary metal-sulfide assemblage. The appearance and chemical compositions of these oxides are similar to

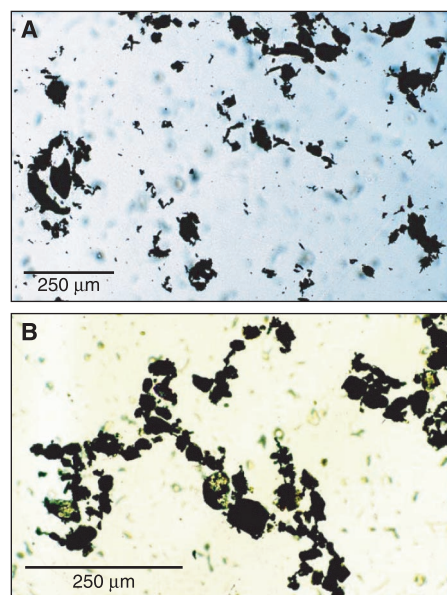


**Fig. 2.** (A) Magnetically separated grains from the end-Permian bed [base of bed 25 (12)] in Meishan, China. The grains shown in plane-polarized light are chemically similar to the Fe-Ni-Si grains reported by Kaiho *et al.* (6) from the same boundary layer. These grains are also similar in appearance to the grains described from the Sasayama P-T boundary layer in Japan (13). Seventy percent of these grains are almost pure Fe (98 to 100%); other metal constituents are Ni (0 to 0.2%), Cr (0 to 0.6%), and Si (0 to 0.39%). (B) The cross-polarized light photomicrograph shows some of the magnetically separated fragments from the P-T boundary layer clay breccia from Graphite Peak, Antarctica. The Fe-rich metal nuggets; Fe,Ni,P,S-bearing oxide grains; and rare Fe,Ni sulfide grains appear dark in this picture. A few silicate and silicate-metal aggregates, which we identified as meteoritic fragments (lower left, middle, and upper right), show characteristic interference colors.

**Table 1.** Chemical composition (averaged) of the silicates from meteoritic fragments discovered in the Graphite Peak P-T boundary layer [sample no. 2060 (8)], with 1 SD. Because of small grain size and uneven surface of the sections, only 29% of analyses yielded totals of 100 ± 1 weight %, with the rest of the analyses totaling between 97.28 and 103.83 weight %. Therefore, all analyses are normalized to 100 weight %, and the average compositions of the oxides and the cations are shown with 1 SD. The analyses of mesostasis (devitrified interstitial glass typically found in chondrules) are of two representative points in the groundmass of a meteoritic fragment. For technical reasons, we did not measure concentrations of TiO<sub>2</sub>, which are typically below detection limit in olivine and low-Ca pyroxene of primitive chondrites (17).

Oxide	Forsterite		Enstatite		Augite		Mn-Augite		Mesostasis	
	n = 17	1σ	n = 19	1σ	n = 7	1σ	n = 2	1σ	n = 1	n = 1
SiO <sub>2</sub>	41.63	0.34	58.98	0.73	54.38	1.03	55.21	0.14	40.64	48.93
Al <sub>2</sub> O <sub>3</sub>	0.10	0.09	1.08	0.90	3.29	1.27	1.80	0.37	9.29	30.47
Cr <sub>2</sub> O <sub>3</sub>	0.37	0.14	0.60	0.20	0.80	0.33	0.84	0.12	0.23	0.00
FeO	0.77	0.34	1.04	0.63	0.56	0.31	0.80	0.07	0.70	0.26
MnO	0.13	0.07	0.14	0.13	0.23	0.18	1.64	0.30	0.21	0.00
MgO	56.77	0.26	36.81	1.18	23.28	2.49	23.59	1.35	44.36	0.78
CaO	0.20	0.12	1.32	0.96	17.44	2.51	16.06	1.95	4.51	19.03
Na <sub>2</sub> O	0.02	0.02	0.02	0.02	0.03	0.03	0.05	0.00	0.06	0.48
K <sub>2</sub> O	0.02	0.03	0.01	0.01	0.00	0.01	0.01	0.02	0.00	0.03
Total	100.00		100.00		100.00		100.00		100.00	100.00
Si	0.982	0.006	1.994	0.015	1.924	0.026	1.960	0.012	1.916	2.250
Al	0.003	0.003	0.051	0.043	0.137	0.053	0.076	0.015	0.516	1.651
Cr	0.007	0.003	0.016	0.005	0.022	0.010	0.024	0.004	0.008	0.000
Fe	0.015	0.007	0.029	0.018	0.017	0.009	0.024	0.002	0.028	0.010
Mn	0.003	0.001	0.004	0.004	0.007	0.005	0.050	0.009	0.008	0.000
Mg	1.997	0.008	1.855	0.050	1.227	0.122	1.248	0.067	3.116	0.054
Ca	0.005	0.003	0.048	0.035	0.662	0.100	0.611	0.076	0.228	0.938
Na	0.001	0.001	0.001	0.001	0.002	0.002	0.004	0.000	0.006	0.043
K	0.000	0.001	0.000	0.001	0.000	0.000	0.001	0.001	0.000	0.002
O	4.000		6.000		6.000		6.000		8.000	8.000
Total cation	3.013	0.005	3.999	0.016	3.997	0.008	3.994	0.004	5.826	4.947

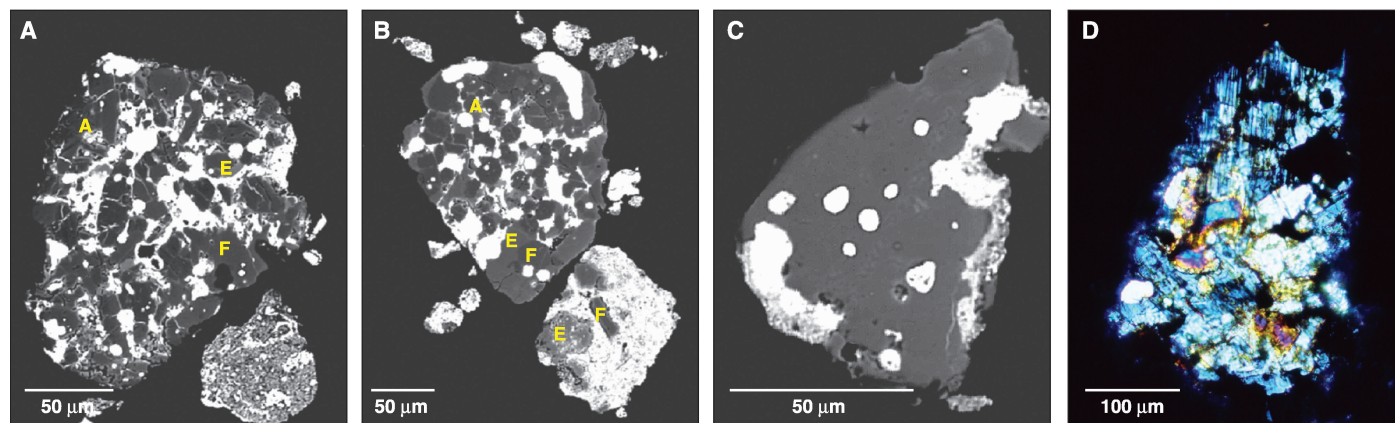


**Fig. 3.** Back-scattered electron (A, B, and C) and cross-polarized light (D) images of representative meteorite fragments from the clay-breccia of the P-T boundary at Graphite Peak, Antarctica: (A) the largest particle consists mainly of pure enstatite (“E”) with poikilitic inclusions of euhedral forsterite (“F”) and interstitial anhedral grains of subcalcic augite (“A”). The abundant Fe,Ni,S,P-bearing oxides (white) form globular masses or veins interstitial to silicates. (B) Two meteoritic particles with different textures. The large particle consists of forsterite crystals (F) enclosed in enstatite (E) with interstitial Ca-bearing pyroxene (A). Globular or irregular masses of Fe,Ni,S,P-bearing oxides (white) are interstitial to silicates. The

matrix (light) of the smaller particle consists mainly of intimate intergrowths of a Fe-rich phyllosilicate (see text for chemical composition), Fe,Ni,S,P-bearing oxides and less abundant pentlandite. (C) The dark gray homogeneous enstatite grain ( $\text{Ca}_{0.08}\text{Fe}_{0.04}\text{Mg}_{1.79}\text{Cr}_{0.03}\text{Al}_{0.06}\text{Si}_{1.98}\text{O}_6$ ) contains euhedral-to-subhedral grains of primary Fe,Ni metal (white). The marginal, irregular masses of Fe,Ni,S,P-bearing oxides are apparently alteration products of the primary metal-troilite assemblage. (D) The parallel, continuous, polysynthetic twinning in the grain with low birefringence allows identification as clinoenstatite. It also shows kink bands.

**Table 2.** Chemical composition (averaged) of opaque phases within the meteorite fragments from the Graphite Peak P-T boundary layer [sample no. 2060 of (8)]. First column, six metal grains of the meteoritic fragments, which totaled between 99 and 101 weight %; second column, 19 metal grains, including the previous 6 grains, with their totals normalized to 100 weight %. The averages in both columns are identical. Fe and Ni oxides include both meteoritic and “loose” grains (Fe,Ni,P,S-oxide grains); next are representative analyses of two sulfide grains, including one troilite, then Fe-Ni-sulfide grains.

Element	Metals				Oxides		Sulfides		
	<i>n</i> = 6	1σ	<i>n</i> = 19	1σ	<i>n</i> = 37	1σ	FeS	(Fe, Ni)S	(Fe, Ni) <sub>9</sub> S <sub>8</sub>
Fe	92.83	0.68	92.97	0.65	56.66	5.62	62.44	59.82	38.93
Ni	5.89	0.31	5.77	0.32	5.33	5.13	0.20	3.09	26.25
Co	0.25	0.04	0.25	0.04	0.21	0.14	0.09	0.31	1.09
Cr	0.49	0.29	0.44	0.22	0.53	0.59	0.02	0.06	0.01
P	0.38	0.19	0.32	0.14	0.43	0.27	0.00	0.00	0.00
Si	0.25	0.35	0.23	0.26	1.12	2.40	0.01	0.13	0.01
S	0.03	0.02	0.01	0.02	1.98	3.08	37.25	36.11	33.70
Total	100.10	0.58	100.00		66.26	3.39	100.01	99.52	100.00

those of discrete Fe,Ni,P,S-oxide grains. Compositionally and texturally similar Fe, Ni,P,S-bearing oxides have been described only in the CM-type chondrites (carbonaceous chondrites of the Mighei-type) (17). The primary Fe,Ni,Co,P-bearing metal has survived only in tiny (typically less than 10 μm), rounded (Fig. 3, A and B) to subhedral (Fig. 3C) grains sealed in forsterite or clinoenstatite. The cosmic Fe/Ni and Co/Ni ratios in these metal grains (Table 2) unequivocally point to meteoritic origin of the grains. Moreover, relatively high concentrations of P, Cr, and Si in these grains, as well as their appearance, are very similar to those in Mg-rich chondrules from the CM chondrites. Rare sulfide grains vary in composition from Ni-poor troilite to Ni-rich pentlandite (Table 2), with most of these grains having compositions of Ni-bearing pyrrhotite. Taken together, the mineralogy

and mineral chemistry of silicates; metal; and Fe,Ni,P,S-bearing oxides point to an affinity of the meteoritic fragments to CM chondrites.

In addition to the olivine-pyroxene-rich meteoritic fragments, there is another type of metal-silicate particle, which consists mainly of very fine-grained intergrowths of a Fe-rich silicate and Fe,Ni-bearing oxides and sulfides, with or without embedded crystal fragments of magnesian silicates (smaller particle in Fig. 3B). The matrix consists mainly of intimate intergrowths of a Fe-rich phyllosilicate ( $\text{SiO}_2 = 24.57$ ,  $\text{Al}_2\text{O}_3 = 2.70$ ,  $\text{FeO} = 46.52$ ,  $\text{MgO} = 11.91$ ,  $\text{CaO} = 1.07$ ); Fe,Ni,S,P-bearing oxides; and less abundant pentlandite. The compositions of the large forsterite (rectangular grain) and enstatite (lighter gray) crystal fragments are identical to those in the large particle. It appears that the small

particle is also of meteoritic origin and may represent a fragment of matrix of a CM chondrite. A number of such small particles were found in the grain mount sections of Graphite Peak.

The fragments we have found are neither interplanetary dust particles (IDP) nor components of the micrometeorite flux. Silicate and metal fragments of modern IDPs are similar to CM chondrites, but they are commonly less than 25 μm in size (18–22). Moreover, the IDPs larger than 50 μm in size are expected to be heavily altered by heating to >1000°C during atmospheric passage (18). The micrometeorites are typically 100 to 400 μm in size, and many are CM chondrites; thus, they overlap with the meteorite fragments from Graphite Peak. The meteorite fragments from Graphite Peak are unusually concentrated in the claystone breccia of Graphite Peak, but are absent from the bed 0.8 m below. Therefore, we conclude that the meteorite fragments from the claystone breccia of Graphite Peak are not part of the regular terrestrial influx of micrometeorites, but represent a separate event.

The meteorite fragments and the discrete Fe-rich metal grains are so well preserved that their preservation must be due to rather unusual circumstances. Great care was taken to prevent laboratory contamination of the samples examined in this study (23), lending support to the natural preservation of these meteoritic fragments in the Antarctic environment. Remarkably fresh appearance of the meteorite fragments (e.g., Fig. 3, A to D) may partly be due to our magnetic separation technique (supporting online material), which involved intense ultrasonification that may have removed surface alterations. Clearly, the Fe-rich metal particles found in the Meishan,



Graphite Peak, and Sasayama samples (13) are not thermodynamically stable in the presence of liquid water, especially at the water-air interface. It appears that a rapid burial in a reducing sedimentary environment is necessary for the survival of metal grains. In the case of Graphite Peak, the presence of meteorite fragments and metal grains in a package of claystone breccia (Fig. 1) above the boundary and at least 25 cm thick indicates rapid burial. Subsequent preservation over millions of years may be attributed to the unique Antarctic environment. Forsterite and clinostannite are also thermodynamically unstable in an H<sub>2</sub>O-rich environment. These minerals might have been protected by the thick rims of matrix phyllosilicates as observed in the CM chondrite parent body that experienced a low-temperature aqueous alteration for tens of million years (17). The causes for the survival of metallic grains and meteorite fragments in the P-T boundary sedimentary beds may not be revealed until these grains and meteorite fragments are studied in situ, that is embedded in their host sediments.

The Fe-Ni-Si metal grains, reported here in association with the chondritic meteoritic fragments in Graphite Peak, are analogous to those found in the Meishan and Sasayama end-Permian sections. At the end-Permian, Antarctica was close to its present position as the southernmost part of Pangaea; south China was at the equator; and Japan was to the north of the equator (24). Such a wide paleogeographic distribution of the Fe-Ni-Si metal grains and their occurrence at the P-T boundary suggests that these grains mark a special event in Earth history and can be used for correlating the P-T boundary sections worldwide. The intimate association of the meteorite fragments with the Fe-Ni-Si grains at Graphite Peak provides further support for an impact-related origin of the Fe-Ni-Si grains as suggested by previous researchers (6, 9, 25).

After the discovery of a large positive iridium anomaly [ $\sim 3$  parts per billion (ppb)] at the K-T boundary caused by the impact of an extraterrestrial body (3), such an anomaly has become the standard test for an impact-related mass extinction event. Samples from the P-T boundary, including the samples studied here, do not exhibit such Ir anomalies [in general the highest values reported are  $< 150$  parts per trillion (ppt) (8)]. The discovery of meteorite fragments in the Graphite Peak P-T boundary section suggests that the presence of an extraterrestrial component at the P-T boundary may not be accompanied by a large Ir anomaly. For example, if all the Ir in the P-T boundary rocks comes from the meteorite fragments only, then the calculated bulk Ir concentration in the claystone breccia will be only  $\sim 10$  ppt, if one considers the mass of chondritic meteorite fragments ( $\sim 40 \mu\text{g}$ ) separated from 2 g of the Graphite Peak sample and assumes the chon-

dritic Ir concentration of  $\sim 500$  ppb in the fragments. If the whole magnetic fraction ( $\sim 1000 \mu\text{g}$ ) is derived from a P-T impactor, then this still would result in an Ir concentration of only 200 ppt. Both values are too low to yield a well-defined Ir anomaly. Inherently heterogeneous character of the claystone breccia in which the extraterrestrial components are found is also an important consideration. Thus, although Ir has been extremely useful for the K-T boundary because of its extreme concentration in a thin layer, it is clear from the evidence presented here that the lack of a large Ir anomaly does not rule out an extraterrestrial component at the P-T boundary.

The mass extinction at the end of the Permian is arguably the greatest in the history of life, when more than 90% of marine species-level extinctions occurred (26, 27), with an equally devastating extinction for plants and animal life on land (28). This coincides with the time of rapid outpouring of the largest known continental flood basalts in Siberia (29–31). Detailed statistical and biostratigraphic analyses (12) in the best-preserved P-T sections in southern China demonstrated the extreme rapidity of this extinction and suggest a catastrophic impact. An extensive search for evidence of impact, such as shocked quartz and Ir anomalies as observed for the K-T boundary, in several P-T sections in Antarctica and Australia (8), did not resolve the issue of an impact at the P-T boundary. Becker *et al.* presented evidence for an impact using fullerenes with trapped extraterrestrial noble gases from P-T boundary sections of south China and Japan, as well as Graphite Peak, Antarctica (9, 11, 25). The fullerene evidence has been challenged (32), and all other potential indicators have been largely ignored (33) because of the low abundances of these tracers (shocked quartz, iridium) in comparison to the K-T boundary, or that the tracer [e.g., Fe-Ni-Si grains in (6)] was considered equivocal because the results did not point directly to an extraterrestrial cause.

The association of discrete metal grains with meteoritic fragments at Graphite Peak P-T boundary as described above, taken together with previous reports of fullerene (9) and shocked quartz grains (8) in the same sample, and the reported occurrence of such metal grains from other P-T localities constitute new criteria for future investigations of the P-T and other boundary layers throughout the geologic record. These observations lead us to believe that continued research on such materials from additional P-T boundary samples will finally lead to a resolution of the long-sought (34) and contentious (32, 33) issue of a catastrophic collision of a celestial body with the Earth at the end-Permian. In light of the new evidence presented here, this is a reasonable interpretation of the global extinction event at the P-T boundary. Thus, it appears to us that the two largest mass extinctions in Earth history at the K-T (2, 35)

and P-T boundaries were both caused by catastrophic collisions with chondritic meteoroids.

#### Reference and Notes

1. F. T. Kyte, F. Langenhorst, F. J. Tepley, *Lunar and Planetary Science XXXI* (abstr. 1811) (2002).
2. F. T. Kyte, *Nature* **396**, 237 (1998).
3. L. W. Alvarez, W. Alvarez, F. Asaro, H. V. Michel, *Science* **208**, 1095 (1980).
4. B. Schmitz, M. Tassinari, B. Peucker-Ehrenbrink, *Earth Planet. Sci. Lett.* **194**, 1 (2001).
5. B. Schmitz, T. Haggerstrom, M. Tassinari, *Science* **300**, 961 (2003).
6. K. Kaiho *et al.*, *Geology* **29**, 815 (2001).
7. E. S. Krull, G. J. Retallack, *Bull. Geol. Soc. Am.* **112**, 1459 (2000).
8. G. J. Retallack *et al.*, *Geology* **26**, 979 (1998).
9. R. J. Poreda, L. Becker, *Astrobiology* **3**, 75 (2003).
10. N. D. Sheldon, G. J. Retallack, *Geology* **30**, 919 (2002).
11. L. Becker, R. J. Poreda, A. G. Hunt, T. E. Bunch, M. Rampino, *Science* **291**, 1530 (2001).
12. Y. G. Jin *et al.*, *Science* **289**, 432 (2000).
13. S. Miono, Y. Nakayama, K. Hanamoto, *Nuclear Instrum. Methods Phys. Res.* **150**, 516 (1999).
14. Magnetic grains were separated from  $\sim 2$  g material of the dark, fine-grained, reddish layer at the base of bed 25 of the Meishan section. These grains of variable size ( $\sim 5$  to  $\sim 300 \mu\text{m}$ ) were mounted on epoxy in glass slides and polished with Al<sub>2</sub>O<sub>3</sub> powder (3, 1, and 0.3  $\mu\text{m}$  size) on a soft woven mat. This polishing process removed many of the finer grains ( $< 20 \mu\text{m}$ ). The remaining grains were examined optically, and many were analyzed with the electron microprobe. The yield of the magnetic grains was  $\sim 0.02\%$ . For the Graphite Peak samples, we followed the same procedure as above. The initial sample size of no. 2060 was  $\sim 50$  g, it was clay-rich material containing substantial amounts of sand-sized minerals and polycrystalline aggregates, which were presorted to a 0.2-g fraction. This sample was not sieved but disaggregated in agate mortars. Magnetic grains from this material were separated with a yield of  $\sim 0.05\%$  of mostly opaque and silicate fragments (for details see supporting online material). Sample no. 315 is similar to sample no. 2060, both in mineral content and texture. This sample was crushed in a stainless steel mortar. About 0.2 g of the crushed rock sample no. 315 was subjected to the same magnetic separation and yielded  $\sim 0.03\%$  meteorite fragments. These grains were mounted, polished and analyzed. Quantitative analysis of the mineral and metal grains was conducted with a JEOL 733 Superprobe at the Harvard-Smithsonian Center for Astrophysics, using wavelength dispersive spectrometers, natural and synthetic metal, and silicate standards. Accelerating voltage, beam current, beam size, and counting time were 15 kV, 20 nA,  $\sim 1 \mu\text{m}$ , and mostly 40 s, respectively.
15. P. R. Renne, Z. Zhang, M. A. Richardson, M. T. Black, A. R. Basu, *Science* **269**, 1413 (1995).
16. S. A. Bowring *et al.*, *Science* **280**, 1039 (1998).
17. A. J. Brearley, R. H. Jones, *Rev. Mineral.* **36**, 3-1 (1998).
18. F. J. M. Rietmeijer, *Rev. Mineral.* **36**, 2-1 (1998).
19. D. E. Brownlee, B. Bates, L. Schramm, *Meteor. Planet. Sci.* **32**, 157 (1997).
20. G. Kurat, C. Koeberl, T. Presper, F. Brandstatter, M. Mauerette, *Geochim. Cosmochim. Acta* **58**, 3879 (1994).
21. W. Beckerling, A. Bischoff, *Planet. Space Sci.* **43**, 435 (1995).
22. E. K. Jessberger *et al.*, in *Interplanetary Dust*, E. Grun, B. Gustafson, S. Dermot, H. Fechtig, Eds. (Springer, Berlin, 2001), pp. 252–294.
23. We can eliminate the possibility that the meteorite fragments and metal grains were found in the samples because of laboratory contamination. We have never crushed or separated any chondritic meteorite in the clean laboratory at the University of Rochester where we separated the magnetic meteorite fragments from the Antarctic samples. We received, on two separate occasions, unprocessed pieces of the similar looking material of sample no. 2060 of the P-T boundary layer clay-

stone breccia from G. Retallack's laboratory. We extracted the magnetic fragments in two separate experiments at Rochester—one for each subsample received. Thus, we repeated our separation twice and in each case we mounted the magnetic fragments on separate glass slides that were later analyzed. From our electron microprobe analyses, the same type of meteorite fragments and the metal nuggets were identified in both subsamples. An important observation is the presence of metal grains in association with the meteorite fragments in the Antarctic samples. These metal grains are neither meteoritic nor are they found in any terrestrial rocks, except that similar metal grains are also found in the P-T boundary at Meishan in China. Most of these metal grains also have compositions that are clearly different from metals used in laboratory tools that may have come in contact with the samples. Also, other similar samples that were not from the P-T boundary but were separated in the same laboratory at the same time did not show these metal particles or meteoritic fragments. Thus, we conclude that it is improbable that the Antarctic P-T sample was contaminated with these metal grains and meteorite fragments.

Later, we obtained yet another rock fragment of no. 2060 (from G. Retallack) with a different (whitish) color from the original pieces (see supporting online material), as well as a different sample no. 315, stratigraphically 23 cm above no. 2060, and received directly from E. Krull. The latter sample also contains meteorite fragments.

24. A. Hallam, P. B. Wignall, *Mass Extinctions and Their Aftermath* (Oxford Univ. Press, New York, 1997).
25. L. Becker, R. J. Poreda, T. E. Bunch, *Proc. Natl. Acad. Sci. U.S.A.* **97**, 2979 (2000).
26. D. M. Raup, *Science* **206**, 217 (1979).
27. D. H. Erwin, *The Greatest Paleozoic Crisis: Life and Death in the Permian* (Columbia Univ. Press, New York, 1993).
28. G. J. Retallack, *Science* **267**, 77 (1995).
29. P. R. Renne, A. R. Basu, *Science* **253**, 176 (1991).
30. I. H. Campbell, G. K. Czamanske, V. A. Fedorenko, R. I. Hill, V. Stepanov, *Science* **258**, 1760 (1992).
31. A. R. Basu *et al.*, *Science* **269**, 822 (1995).
32. K. A. Farley, S. Mukhopadhyay, *Science* **293**, 2343a (2001).
33. C. Koeberl, I. Gilmour, W. E. Reimold, P. Claeys, B. Ivanov, *Geology* **30**, 855 (2002).
34. Y. Sun *et al.*, "The discovery of an iridium anomaly in

the Permian-Triassic boundary clay in Changxing, Zhejiang, China, and its significance," 27th International Geological Congress (Science Press, Beijing, 1984).

35. A. Shukolyukov, G. W. Lugmair, *Science* **282**, 927 (1998).
36. We are grateful to G. J. Retallack and E. Krull for providing the Graphite Peak samples from Antarctica and to S. D'Hondt for the Meishan, base 25, ferruginous sample from China that was collected in collaboration with D. H. Erwin and Y. G. Jin. Research supported by the Division of Earth Sciences (EAR), NSF (A.R.B.); the Division of Ocean Sciences (OCE), NSF (L.B. and R.J.P.); NASA (Exobiology, L.B.); and NASA (Origin of Solar System and Cosmochemistry, S.B.J.) grants.

**Supporting Online Material**

www.sciencemag.org/cgi/content/full/302/5649/1388/DC1

Materials and Methods

Figs. S1 and S2

Tables S1 to S4

References and Notes

26 August 2003; accepted 6 October 2003

# Chemostratigraphic Evidence of Deccan Volcanism from the Marine Osmium Isotope Record

G. Ravizza<sup>1\*</sup> and B. Peucker-Ehrenbrink<sup>2</sup>

Continental flood basalt (CFB) volcanism is hypothesized to have played a causative role in global climate change and mass extinctions. Uncertainties associated with radiometric dating preclude a clear chronological assessment of the environmental consequences of CFB volcanism. Our results document a 25% decline in the marine <sup>187</sup>Os/<sup>188</sup>Os record that predates the Cretaceous-Tertiary boundary (KTB) and coincides with late Maastrichtian warming. We argue that this decline provides a chemostratigraphic marker of Deccan volcanism and thus constitutes compelling evidence that the main environmental consequence of Deccan volcanism was a transient global warming event of 3° to 5°C that is fully resolved from the KTB mass extinction.

Flood basalt volcanism continues to be considered as a cause of several mass extinctions (1), including the end-Guadalupian, the end-Permian, the end-Triassic, and the early Jurassic extinctions (2). If flood basalt eruption played a causative role in an extinction event, then major volcanism should have immediately preceded extinction. Though this criterion is simply stated, uncertainties associated with radiometric dating of flood basalts make it difficult to test.

In the specific case of the Deccan Flood Basalts, uncertainties associated with the age and duration of volcanism have given

rise to conflicting conclusions regarding the environmental consequences of these eruptions. Several paleoclimate studies assert that Deccan volcanism was responsible for a warming event several hundred thousand years before the KTB (3–5). However, existing age constraints are only permissive of this interpretation. Most recent efforts to refine the chronology of Deccan volcanism conclude that the major phase of volcanism was effectively coincident with the KTB and may have contributed to the extinction event (6, 7).

Recent results suggest that the marine Os isotope record can provide evidence of flood basalt eruption in the marine sedimentary record (8). In the modern ocean, dissolved Os is nearly homogenous, with an <sup>187</sup>Os/<sup>188</sup>Os ratio of 1.06, and it is accurately preserved by recent marine sediments in several depositional settings (9). At any given time, seawater <sup>187</sup>Os/<sup>188</sup>Os

reflects a balance between average riverine input (<sup>187</sup>Os/<sup>188</sup>Os ≈ 1.3) and mantle and extraterrestrial inputs (<sup>187</sup>Os/<sup>188</sup>Os ≈ 0.13) to the global ocean (9). Recently, Os isotope data have been used to argue that an abrupt decline in seawater <sup>187</sup>Os/<sup>188</sup>Os just before the Triassic-Jurassic boundary marked the onset of volcanic activity in the Central Atlantic magmatic province (8). The rationale for this argument is based on the idea that weathering of these young, mantle-derived basalts released substantial quantities of unradiogenic Os (Os with a low <sup>187</sup>Os/<sup>188</sup>Os ratio) to the global ocean. The short marine residence time of Os allows whole-ocean shifts in isotope composition to occur on time scales of about 10,000 years (9), giving the marine Os isotope record the fidelity required to serve as a clear stratigraphic marker of the initiation of major flood basalt volcanism. This is analogous to local minima and inflections in the marine <sup>87</sup>Sr/<sup>86</sup>Sr record that are associated with emplacement and weathering of flood basalt provinces (10).

Existing data (11) suggest that a similar shift in the marine <sup>187</sup>Os/<sup>188</sup>Os record may be associated with Deccan volcanism. However, the close temporal association of Deccan volcanism with the KTB complicates the recognition of such a shift. As extraterrestrial materials and young basalts have similar <sup>187</sup>Os/<sup>188</sup>Os ratios (9), there is no means of resolving these two components if they are truly contemporaneous. Two aspects of an existing, low-resolution Os isotope record of the KT transition suggest a source of unradiogenic Os unrelated to the KTB impact. First, the decline in <sup>187</sup>Os/<sup>188</sup>Os begins several meters below the Ir anomaly that defines the KTB in this core (Fig. 1). Second, it is difficult to reconcile the overall structure of the Os iso-

<sup>1</sup>Department of Geology and Geophysics, University of Hawaii, Honolulu, HI 96822–2225, USA. <sup>2</sup>Department of Marine Chemistry and Geochemistry, Woods Hole Oceanographic Institution (WHOI), Woods Hole, MA 02543, USA.

\*To whom correspondence should be addressed. E-mail: ravizza@hawaii.edu